Chinese Journal of
POLYMER SCIENCE

ARTICLE

https://doi.org/10.1007/s10118-021-2582-3
Chinese J. Polym. Sci. **2021**, *39*, 1392–1402

Monoclonal Antibody-conjugated Polyphosphoester-*hyd*-DOX Prodrug Nanoparticles for Targeted Chemotherapy of Liver Cancer Cells

Ya-Kui Huang[a], Hong-Rui Tian[a], Ming-Zu Zhang[a], Jin-Lin He[a], Jian Liu[b], and Pei-Hong Ni[a*]

[a] *College of Chemistry, Chemical Engineering and Materials Science, State and Local Joint Engineering Laboratory for Novel Functional Polymeric Materials, Jiangsu Key Laboratory of Advanced Functional Polymer Design and Application, Suzhou Key Laboratory of Macromolecular Design and Precision Synthesis, Soochow University, Suzhou 215123, China*
[b] *Institute of Functional Nano and Soft Materials (FUNSOM), Soochow University, Suzhou 215123, China*

Electronic Supplementary Information

Abstract In order to overcome the limitation of traditional active nano-therapeutic drugs on tumor targeting efficiency which cannot reach the receptor/target in sufficient amount in the body, in this work, we developed a monoclonal antibody (mAb) and a polymer-*hyd*-doxorubicin prodrug conjugate, which enables the self-assembled nanoparticles to have precise targeting, tumor tissue aggregation and pH-sensitive drug release. We first prepared an amphiphilic polymer prodrug, abbreviated as H_2N-PEEP-*b*-PBYP-*hyd*-DOX, *via* a combination of ring-opening polymerization (ROP) and "click" chemistry, in which PEEP and PBYP represent two kinds of phosphoester segmemts, *-hyd-* is hydrazone bond. After self-assembly into prodrug nanoparticles (PDNPs) with a diameter of about 93 nm, CD147 mAb was conjugated onto the PDNPs by EDC/NHS chemistry to form mAb-PDNPs. For the PDNPs and mAb-PDNPs, we also investigated their stability, *in vitro* drug release behavior and cellular uptake. The results showed that the pH-responsive PDNPs can remain relatively stable under the condition of PB 7.4 buffer solution. However, under acidic conditions or in the presence of phosphodiesterase I (PDE I), both the amount and rate of DOX release increased at the same incubation period. Cytotoxicity assay showed that mAb-PDNPs exhibited higher cytotoxicity (IC_{50}: 1.12 mg·L^{-1}) against HepG2 cells than PDNPs (IC_{50}: 2.62 mg·L^{-1}) without monoclonal antibody. The nanoparticles with antibodies mAb-PDNPs have relatively better stability and can directly achieve the targeting drug delivery through CD147 mAb.

Keywords Monoclonal antibody; Polymeric prodrug; Polyphosphoester; Drug delivery; Targeted therapy

Citation: Huang, Y. K.; Tian, H. R.; Zhang, M. Z.; He, J. L.; Liu, J.; Ni, P. H. Monoclonal antibody-conjugated polyphosphoester-*hyd*-DOX prodrug nanoparticles for targeted chemotherapy of liver cancer cells. *Chinese J. Polym. Sci.* **2021**, *39*, 1392–1402.

INTRODUCTION

In recent years, cancer incidence and death rates have increased rapidly worldwide, with liver cancer being the fifth most common cancer and the second most common cause of cancer-related death worldwide. In a 2020 global tally of cancer patients, liver cancer accounted for 6.3% of all cases and 10.1% of deaths.[1,2] Traditional cancer treatment methods mainly include surgery, chemotherapy, immunotherapy and nano drug therapy.[3,4] Chemotherapy is the option of most patients in certain procedures because of good therapeutic effect. However, traditional chemotherapy has some limitations, mainly including nonspecific selectivity, poor bioavailability, rapid blood/renal clearance, less accumulation of drug in tumor site, serious multi-drug resistance (MDR) and side effects for health organization.[5,6] Therefore, researchers focus on developing new drug carriers and delivery methods to improve the water solubility of antitumor drugs, enabling them to achieve long-term circulation in the body and ultimately to target to the tumor tissue for drug release.

Antibody-drug conjugates (ADCs) have become a research hotspot and an important development direction in the field of targeted tumor therapy. In this method, small molecules as linkers are used to covalently couple highly toxic drugs with monoclonal antibodies, in which monoclonal antibodies can target to recognize antigens and achieve targeted drug delivery.[7,8] To date, eight kinds of ADC drugs have been approved by the Food and Drug Administration (FDA) and more than 100 are currently in separate phases of clinical trials, with much more planned in the future.[9,10] Although ADC drugs show good safety and effectiveness in clinical application, the toxins used are usually much toxic, such as maytansine and dolastoxin. Therefore, if the toxins are released in advance of the phase of circulation in the body, significant damage to

* Corresponding author, E-mail: phni@suda.edu.cn
Received February 25, 2021; Accepted March 19, 2021; Published online June 25, 2021

human health tissue would be caused.[11,12] Usually, these highly toxic drugs have poor water solubility, and will still cause a large amount of aggregation *in vivo* after conjugation with antibodies, thus reducing the therapeutic effect.[13,14] Accordingly, it is very urgent to develop a conjugation technology with stable and effective antibodies and drugs.

To overcome the deficiency of chemotherapeutic drugs, researchers have proposed various prodrug strategies, that is, combination of chemotherapeutic drugs with carriers.[15,16] Amphiphilic polymer nanoparticles, water-soluble polymers, vesicles, liposomes and inorganic nanomaterials have been used as drug carriers.[17–20] Polymeric prodrug system is considered as a promising drug delivery strategy, which refers to the coupling of a physiologically active and transportable polymer carrier with oncology drugs. In addition, the carrier can be removed through simple hydrolysis or enzymatic hydrolysis in the process of internal circulation to realize the accumulation of drugs in tumor.[21,22] For example, Liu *et al*. reported a promising polyprodrug amphiphile which can self-assemble into four types of uniform nanostructures. This strategy can covalently tether repeating prodrug units and deliver high-dosage parent drug at lesion sites, possessing flexible design of polymer topologies, self-assembling morphologies and theranostic functions.[23,24] Other researchers have also proposed valuable strategies for the design of prodrugs.[25,26]

Substituting polymers for small molecules as ADC linkers can enhance drug binding reaction sites and prevent the use of highly toxic drugs, thereby using less toxic anticancer drugs. This product that combines antibodies with antitumor drugs through polymers is called antibody-polymer-drug conjugation (APDC).[27–29] In recent years, the reported polymers mainly include poly(ethylene glycol) (PEG),[30] polycaprolactone (PCL),[31] hyaluronic acid (HA)[32] and polyphosphoesters (PPEs).[33] If polymer carriers are bonded with antitumor drugs by stimulating responsive chemical bonds, they will remain stable in normal human tissues or blood environment, while break under tumor microenvironment conditions to release the active drug.[34,35] It is known to all that biocompatibility and biodegradability are two key points in the selection of carriers. Our group reported a variety of stimuli-responsive polymer prodrugs using polyphosphoesters as the carriers. Compared with natural macromolecules, the side chain of polyphosphoesters is easy to functionalize and has good biocompatibility and biodegradation.[36–38] Therefore, polyphosphoesters as drug carriers hold a good application prospect.

Different cancer cells may have different overexpressed receptors, so it is necessary to select target molecules that can bind specifically to the overexpressed receptors. At present, the target molecules reported in literature mainly include monoclonal antibodies,[29,39] peptide,[40] hyaluronic acid (HA) and folic acid (FA).[41] CD147 mAb is a transmembrane glycoprotein belonging to the immunoglobulin superfamily. It is worth mentioning that CD147 mAb plays an important role in the progression, invasion and metastasis of tumors. In addition, it is highly expressed on the surface of hepatoma carcinoma cells.[42,43] The fragment from CD147 mAb, called metuximab, was approved for using in liver cancer patients in China in 2005.[44] So it is feasible to select CD147 mAb as a targeted molecule for the treatment of liver cancer.

Herein, we selected CD147 mAb as the targeted molecules and polyphosphoester as the drug carrier, aiming to achieve the targeted release of DOX at the tumor site, so as to reduce the systemic toxic and side effects. At first, an amphiphilic diblock copolymer precursor BocNH-PEEP-*b*-PBYP was synthesized by using EABoc as initiator to initiate the ring-opening polymerization (ROP) of two kinds of phosphoester monomers, EOP and BYP, in turn. After the BocNH-group was deprotected by hydrolysis, a pH-sensitive prodrug H_2N-PEEP-*b*-PBYP-*hyd*-DOX was prepared by Cu(I)-catalyzed azide-alkyne cycloaddition (CuAAC) "click" reaction between the alkynyl of H_2N-PEEP-*b*-PBYP and a doxorubicin-azide derivative (DOX-*hyd*-N_3). Subsequently, the prodrug could self-assemble into nanoparticles, which are modified with CD147 mAb on the surface. The nanoparticles with antibodies are expected to achieve targeted drug release in tumor cell microenvironment, as shown in Scheme 1. Compared with normal cells, tumor cells possess an acidic environment and higher concentration of phosphodiesterase I (PDE I), which enables the hydrazone bond on the prodrug and the PPE linkage on the precursor polymer chain to break quickly and release DOX, so as to realize the inhibition ability of tumor. This work provides a simple preparation method of nanoparticles based on PPEs, which is stable in the internal circulation and can achieve targeted therapy.

RESULTS AND DISCUSSION

Characterization of the H_2N-PEEP-*b*-PBYP-*hyd*-DOX

In this study, a polymeric prodrug based on polyphosphoesters was prepared by the following steps and the synthesis routes were shown in Scheme 2. Firstly, the polyphosphoester containing EABoc fragment at one end was prepared *via* one-pot sequential feeding of EOP and BYP monomers by ROP, using 2-(*tert*-butoxycarbonylamino)-1-ethanol (EABoc) as initiator. Secondly, an amino-terminated polyphosphoester H_2N-PEEP-*b*-PBYP was obtained by hydrolysis. Then, DOX-*hyd*-N_3 was prepared and conjugated to the backbone *via* "click" chemistry between the alkynyl group of PBYP segment and azide group of DOX-*hyd*-N_3. Finally, we got the polymeric prodrug H_2N-PEEP-*b*-PBYP-*hyd*-DOX. The detailed experimental process is described in the electronic supplementary information (ESI).

In order to confirm the chemical structures and the molecular weights of the diblock copolymers, we have made the following characterizations: ^{31}P-NMR, GPC, ^{1}H-NMR, FTIR, UV-Vis and HPLC analysis, respectively. The derivative DOX-*hyd*-N_3, monomers EOP and BYP were separately prepared. Figs. S1, S2 and S3 in ESI prove that the required DOX derivative and monomers have been synthesized. Fig. S4(A) (in ESI) is the ^{31}P-NMR spectrum of the BocNH-PEEP product after 60 min of EOP polymerization, indicating that all EOP monomers have been polymerized completely. In Fig. S4(B) (in ESI), the appearance of the new peak assigned to the PBYP repeat units indicates the successful synthesis of BocNH-PEEP-*b*-PBYP. From the GPC traces (Fig. 1), we can further confirm the successful synthesis of the diblock copolymer due to the increase of molecular weight.

https://doi.org/10.1007/s10118-021-2582-3

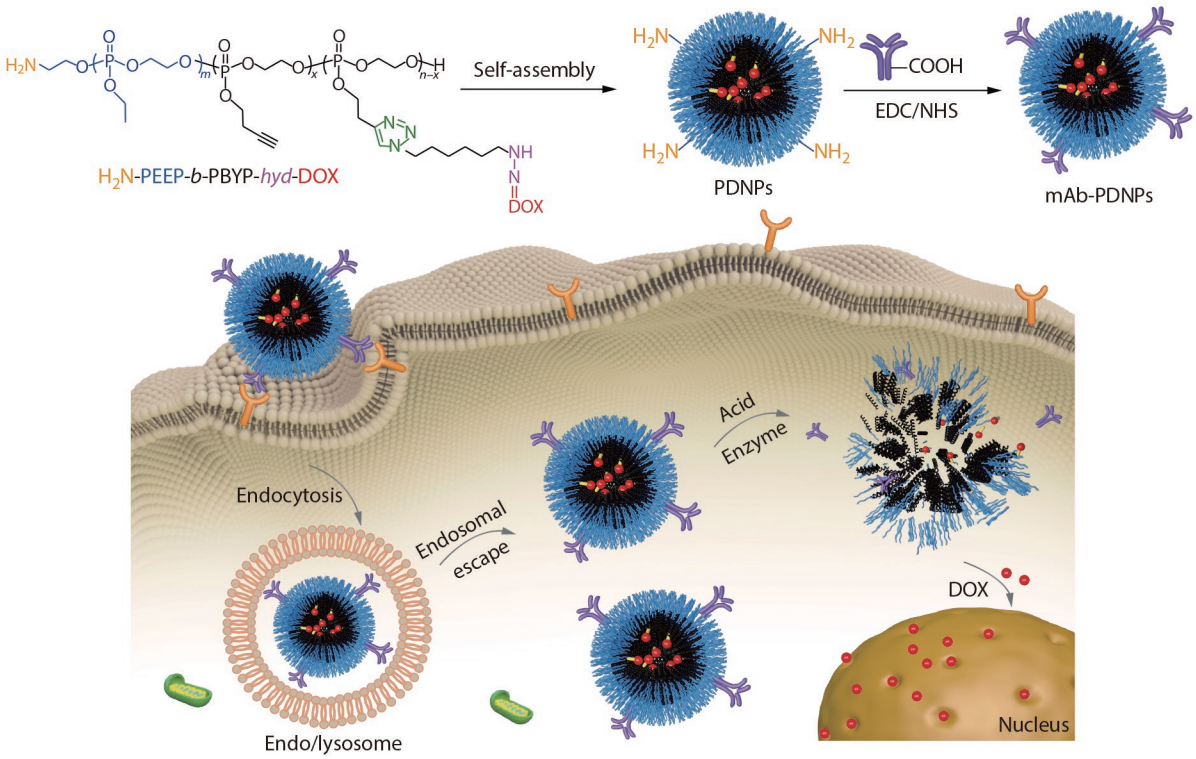

Scheme 1 Schematic illustration of mAb-PDNPs formed from the self-assembly of H_2N-PEEP-*b*-PBYP-*hyd*-DOX prodrug and the drug delivery under the microenvironment of tumor cells.

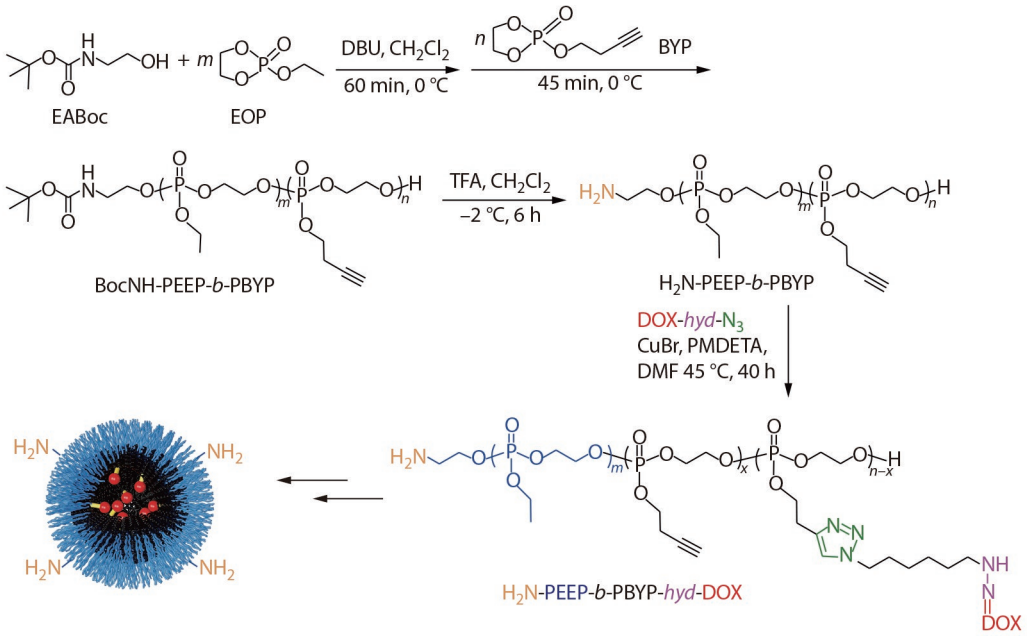

Scheme 2 Synthesis routes to polymeric prodrug H_2N-PEEP-*b*-PBYP-*hyd*-DOX.

In addition, the results of ^{1}H-NMR spectra in Fig. 2 indicate that we have obtained the precursors BocNH-PEEP, BocNH-PEEP-*b*-PBYP, H_2N-PEEP-*b*-PBYP and the prodrug H_2N-PEEP-*b*-PBYP-*hyd*-DOX, respectively. In Fig. 2(A), the chemical shift peaks at δ=1.43 ppm (peak a), δ=1.34 ppm (peak f), δ=4.33–4.22 ppm (peak h) and δ=4.22–4.12 ppm (peak e) show that the polymer BocNH-PEEP was synthesized. In Fig. 2(B), the new characteristic peaks at δ=2.04 ppm (peak g) and δ=2.61 ppm (peak i) indicate that the diblock copolymer BocNH-PEEP-*b*-PBYP was obtained. In Fig. 2(C), the chemical shift at δ=8.59 ppm (peak k) indicates the appearance of the amino group at one end of the copolymer chain after hydro-

https://doi.org/10.1007/s10118-021-2582-3

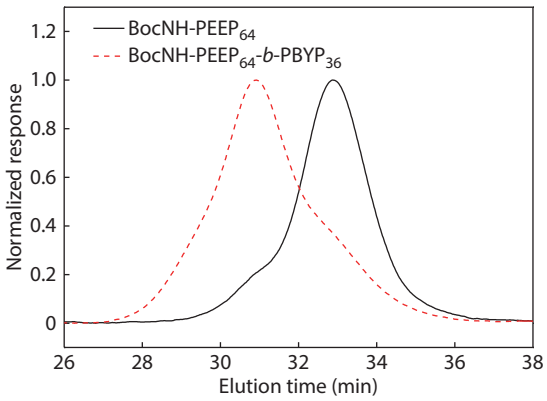

Fig. 1 GPC traces of BocNH-PEEP$_{64}$ ($\overline{M}_n$=1.25×10^4 g·mol^{-1}, $Đ$=1.05) and BocNH-PEEP$_{64}$-*b*-PBYP$_{36}$ ($\overline{M}_n$=1.69×10^4 g·mol^{-1}, $Đ$=1.09), the number of repeating units is calculated by ^{1}H-NMR spectra.

lysis. After click reaction between H_2N-PEEP-*b*-PBYP and DOX-*hyd*-N_3, the characteristic signal (peak q) that appears at δ=7.55 ppm in Fig. 2(D) prove that the prodrug H_2N-PEEP-*b*-PBYP-*hyd*-DOX have been prepared successfully. On the basis of ^{1}H-NMR spectrum in Fig. 2(B), the degree of polymerization of both PEEP (x) and PBYP (y) can be calculated by the following Eqs. (1) and (2):

$$x = \frac{3A_f}{A_a} \quad (1)$$

$$y = \frac{9A_g}{A_a} \quad (2)$$

where A_a is the integral area of the protons at δ=1.43 ppm in BocNH— (peak a, —C$\underline{H}_3$), A_f is the integral area of the protons at δ=1.34 ppm in PEEP chain segment (peak f, —C$\underline{H}_3$) and A_g is the integral area of the protons at δ=2.04 ppm in PBYP chain segment (peak g, —$CH_2C{\equiv}C\underline{H}$).

Furthermore, the molecular weights of BocNH-PEEP and BocNH-PEEP-*b*-PBYP could be calculated by Eqs. (3) and (4), in which 152.01 and 176.11 represent the molecular weights of one repeating unit of PEEP and PBYP, respectively, 144 is the molecular weight of EABoc. The data of molecular weights ($\overline{M}_n$) and molecular weight distributions ($Đ$) of copolymers are listed in Table 1. Considering the experimental effect of assembly, we chose BocNH-PEEP$_{64}$-*b*-PBYP$_{36}$ for follow-up experiments.

$$\overline{M}_{n\,(\text{BocNH-PEEP})} = 152.01x + 144 \quad (3)$$

$$\overline{M}_{n\,(\text{BocNH-PEEP-}b\text{-PBYP})} = \overline{M}_{n\,(\text{BocNH-PEEP})} + 176.11y \quad (4)$$

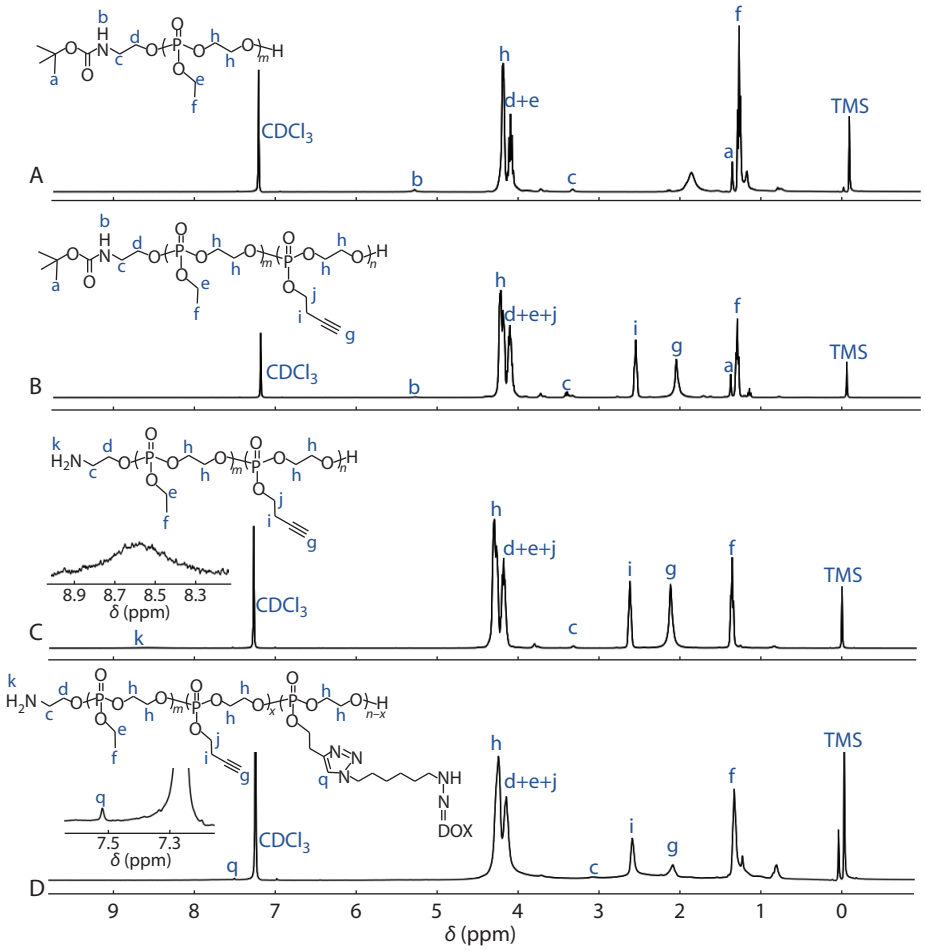

Fig. 2 ^{1}H-NMR spectra of (A) BocNH-PEEP$_{64}$, (B) BocNH-PEEP$_{64}$-*b*-PBYP$_{36}$, (C) H_2N-PEEP$_{64}$-*b*-PBYP$_{36}$ and (D) H_2N-PEEP$_{64}$-*b*-PBYP$_{36}$-*hyd*-DOX.

https://doi.org/10.1007/s10118-021-2582-3

Table 1 Molecular weights and molecular weight distributions of BocNH-PEEP and BocNH-PEEP-*b*-PBYP.

Sample	$\overline{M}_n$ [a] (g·mol^{-1})	$\overline{M}_n$ [b] (g·mol^{-1})	$\overline{M}_w$ [b] (g·mol^{-1})	$Đ$ [b]
BocNH-PEEP$_{64}$	9700	12500	13300	1.05
BocNH-PEEP$_{64}$-*b*-PBYP$_{36}$	16000	16900	18400	1.09
BocNH-PEEP$_{30}$-*b*-PBYP$_{23}$	8600	7500	10600	1.41
BocNH-PEEP$_{30}$-*b*-PBYP$_{30}$	8500	9600	10800	1.13
BocNH-PEEP$_{45}$-*b*-PBYP$_{30}$	9100	9900	10900	1.10

[a] Calculated from ^{1}H-NMR spectra. (solvent: $CDCl_3$); [b] Measured by GPC. (eluent: DMF; standard: polystyrene).

FTIR, UV-Vis and HPLC were also measured to prove the successful preparation of the prodrug H_2N-PEEP-*b*-PBYP-*hyd*-DOX. The characteristic absorption at 2105 cm^{-1} ($\nu_{-C\equiv CH}$) in Fig. S5(B) (in ESI) indicate the successful synthesis of the copolymer BocNH-PEEP-*b*-PBYP. The characteristic absorption at 3280 cm^{-1} (ν_{-NH_2}) and 1673 cm^{-1} (ν_{-NH_2}) in Fig. S5(C) (in ESI) confirm the amino group at the end of the copolymer was obtained. The disappearance of the characteristic absorption at 2105 cm^{-1} ($\nu_{-C\equiv CH}$) shows that the prodrug H_2N-PEEP-*b*-PBYP-*hyd*-DOX has been synthesized. What's more, as shown in the Fig. S6 (in ESI), there is a significant red shift between the H_2N-PEEP-*b*-PBYP-*hyd*-DOX and DOX in the UV-Vis spectrum. Therefore, it can illustrate that DOX has been bound to the side groups of the copolymer. DOX, DOX-*hyd*-N_3 and H_2N-PEEP-*b*-PBYP-*hyd*-DOX were measured by HPLC and showed different retention time (Fig. S7 in ESI), thus proving that the required prodrugs have been synthesized.

Self-Assembly Behavior of H_2N-PEEP-*b*-PBYP-*hyd*-DOX

The prodrug H_2N-PEEP-*b*-PBYP-*hyd*-DOX is an amphiphilic copolymer, which can self-assemble into nanoparticles (abbreviated as PDNPs) with the PBYP chain segment and the hydrophobic DOX as the core, and the PEEP chain segment as the shell in aqueous solution. The critical aggregation concentration (CAC) can be used to evaluate the self-assembly capability of amphiphilic polymers.[45] In general, the low CAC value means that the copolymer can form nanoparticles at low concentration. We used the pyrene fluorescence probe method for measuring the fluorescence intensity of a series of concentrations of polymer solutions. Fig. S8 (in ESI) shows the relationship between the logarithm of the concentration of the copolymer solution (log*C*) and the ratio of the fluorescence intensity of the third peak to the first peak (I_3/I_1), and the CAC value (0.096 mg·mL^{-1}) of H_2N-PEEP-*b*-PBYP-*hyd*-DOX is obtained by intersecting the two straight lines.

The average particle size ($\overline{D}_Z$) and size polydispersity index (size PDI) are two key parameters for the delivery of polymer prodrug. It has been reported that the nanoparticles in the range of 50–200 nm can be transported to the tumor tissue effectively.[46] In this study, we characterized the particle sizes and the morphologies by DLS and TEM measurements. From Fig. 3(a) we can get the result that the prodrug H_2N-PEEP-*b*-PBYP-*hyd*-DOX can self-assemble into nanoparticles with uniform particle size in aqueous solution. The average particle size of PDNPs is about 70 nm. Fig. 3(b) shows the particle size distribution histogram of H_2N-PEEP-*b*-PBYP-*hyd*-DOX (0.5 mg·mL^{-1}) with particle size of 93 nm and size PDI of 0.092. The average particle size measured by DLS is larger than that observed by TEM, which is mainly because the average particle size of nanoparticles with hydrophilic chains is different in the aqueous solution and the dry environment. After the surface of polymer prodrug nanoparticles was combined with monoclonal antibody, namely mAb-PDNPs, the particle morphology and particle size distribution histogram are shown in Figs. 3(c) and 3(d). The slight increase in particle size is due to the binding of CD147 monoclonal antibodies to the surface of PDNPs, forming mAb-PDNPs. When the PDNPs were exposed to the environment of PB 5.0 buffer for 48 h, the original self-assembled nanoparticles almost dissociated, and no spherical particles were observed, as shown in Fig. 3(e). And the corresponding particle size distribution becomes wider (Fig. 3f), which means that the polymeric prodrug has acid-sensitiveness.

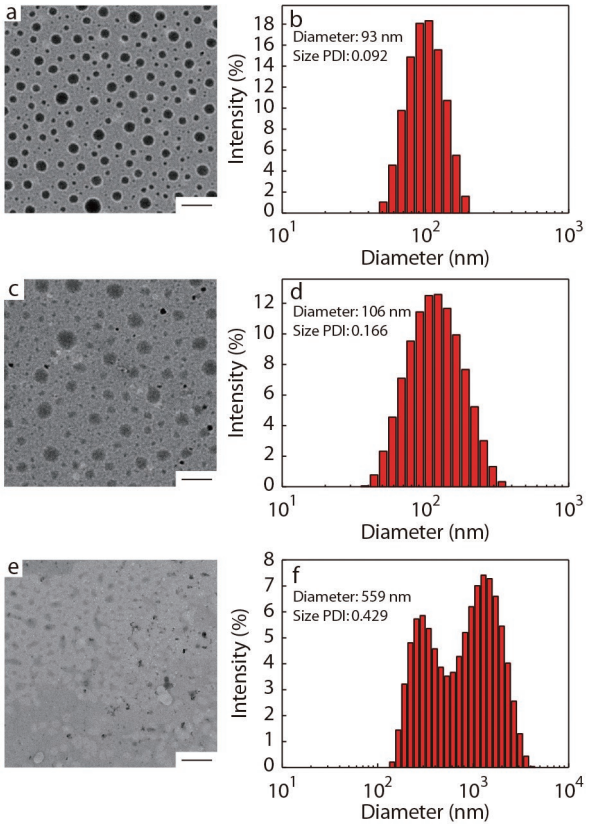

Fig. 3 TEM images of the nanoparticles: (a) PDNPs in PB 7.4 after 48 h; (c) mAb-PDNPs in PB 7.4 and (e) PDNPs in PB 5.0 after 48 h. (b, d and f) Particle-size distribution histograms of the samples in panels (a), (c) and (e), respectively. All the micellar concentrations were kept at 0.5 mg·mL^{-1}; the scale bars of images are 200 nm.

Characterization of CD147-PEEP-*b*-PBYP-*hyd*-DOX

To confirm whether the CD147 mAb was successfully bound to PDNPs, XPS was measured for elemental analysis of the two samples, PDNPs and mAb-PDNPs, as shown in Fig. S9 (in ESI). Since PDNPs do not contain sulfur, and antibody contains disulfide bond, the sulfur peak in the XPS spectrum (Fig. S9B in ESI) indirectly proves that CD147 mAb has been attached to the

https://doi.org/10.1007/s10118-021-2582-3

surface of prodrug nanoparticles PDNPs.

In addition, in the FTIR spectum of Fig. S10 (in ESI), the migration of the carbonyl absorption peak from 1665 cm^{-1} to 1638 cm^{-1} can also account for the coupling of CD147 mAb to PDNPs. To further test the modification rate of CD147 mAb, different batches of samples were tested by BCA protein kit to determine the modification rate of CD147 mAb and the results are shown in Table 2. By measuring the zeta potential of the particle, it can also be proved that the antibody binds to the prodrug nanoparticle. Due to the amino groups on the surface of the prodrug nanoparticles, the zeta potential of PDNPs was +7.3 mV. When the monoclonal antibody CD147 mAb was linked to PDNPs, the amino group on the surface of the PDNPs will be consumed, the zeta potential would gradually decrease. Considering the experimental effect and cost, the sample with a mass ratio of CD147 mAb to PDNPs of 4 (CD147 mAb : PDNPs, μg/mg) was chosen for the subsequent experiments.

Table 2 CD147 mAb content and zeta potential in mAb-PDNPs before and after the binding reaction, in which the mass ratio of CD147 mAb to PDNPs is μg/mg.

Entry	CD147 mAb added (μg/mg)	Zeta potential (mV)	CD147 mAb modified (μg/mg)
PDNPs	–	+7.3	–
mAb-PDNPs-1	2	+6.2	1.2±0.114
mAb-PDNPs-2	4	+4.0	2.3±0.152
mAb-PDNPs-3	2.5	–	1.7±0.127
mAb-PDNPs-4	5	–	2.6±0.161

Enzymatic Degradation

In the presence of phosphodiesterase I (PDE I) and PB 7.4 buffer solution, a degradation experiment on the diblock copolymer H_2N-$PEEP_{64}$-*b*-$PBYP_{36}$ was performed. The process of degradation was monitored by ^{1}H-NMR spectroscopy. As shown in Fig. 4, we could get the results that the original peaks assigned to protons of the PEEP and PBYP blocks gradually weakened or disappeared along with the incubating time from 0 h to 72 h, and several new signals appeared at δ=0.83 ppm, δ=1.25 ppm, and δ=1.33 ppm, respectively. Therefore, the polyphosphoesters as the main chain have good biodegradability.

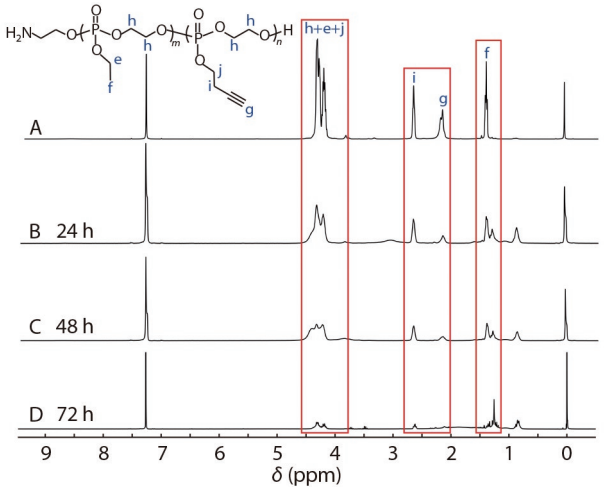

Fig. 4 ^{1}H-NMR spectra of (A) H_2N-$PEEP_{64}$-*b*-$PBYP_{36}$ and its degradation products at predetermined time intervals for (B) 24 h, (C) 48 h and (D) 72 h, respectively. (Solvent: $CDCl_3$).

Particle Stability and pH Sensitivity

The nanoparticles PDNPs formed by self-assembly of amphiphilic polymer prodrug in water should remain stable in the normal *in vivo* environment. When entering the tumor cell microenvironment, due to the internal weak acidity, the hydrazone bond is broken, the nanoparticles would dissociated and DOX be released.[38] These processes can be confirmed by observing the changes of particle size ($\overline{Dz}$) and size PDI of the polymer prodrug nanoparticles under specific conditions. As shown in Figs. 5(a) and 5(b), there were inconspicuous changes of the particle size over 48 h, that can illustrate the favorable stability of PDNPs under neutral conditions. However, under the condition of PB 6.0 and PB 5.0 buffer, the particle size and size PDI of PDNPs gradually increased with time, which indicate that PDNPs will disintegrate through hydrazone bond in weakly acidic medium and effectively release drug. At the same time, combined with the results of the enzymatic degradation of the polyphosphoester backbond, we can believe that the prepared polymeric prodrug nanoparticles have good pH-responsiveness and drug release performance in the tumor microenvironment.

In Vitro Release of DOX

In recent years, pH-responsive polymers are playing an increasingly important role in drug delivery system.[47–49] In this study, as a performance acid-sensitive bond, the hydrazone bond will ensure efficient release of the DOX under acidic conditions while maintaining equilibrium under physiological conditions. The cumulative DOX release experiments *in vitro* were performed in different conditions: (A) PB 5.0, (B) PB 6.0, (C) PB 7.4 with PDE I, (E) PB 7.4 for PNDPs, and (D) PB 7.4 for mAb-PDNPs, respectively, to investigate the release of DOX, as shown in Fig. 6. We can see that after 50 h of incubation in thermostatic oscillator, the cumulative release of DOX was up to 65% for PDNPs under the condition of PB 5.0 buffer (Curve A), while 10% of DOX release for both PDNPs and mAb-PDNPs after 50 h of incubation in PB 7.4 buffer, indicating that mAb-PDNPs have similar stability to PDNPs in normal physiological environment. By comparing Curve D with Curve E, we can know that the modification of CD147 mAb on the surface of prodrug nanoparticles has little effect on the release of DOX. Furthermore, in the presence of PDE I, PDNPs would dissociate and release DOX, as shown in Curve C. These results indicate that the prodrug nanoparticles PDNPs can release DOX by dissociation under acidic conditions and the polyphosphoesters have good biodegradability.

Biocompatibility

The biocompatibility of materials is one of the important bases to evaluate whether they can be used as drug carriers in drug delivery system. In this study, methyl thiazolyl tetrazolium (MTT) assays were used to study the cytotoxicity of the polymer H_2N-PEEP-*b*-PBYP against human umbilical vein endothelial cells (HUVEC cells), mouse fibroblast cells (L929 cells) and human hepatocellular carcinomas cells (HepG2 cells), respectively. These cells were incubated with different concentrations of polymer solution for 48 h. Fig. 7 illustrates that the viability of

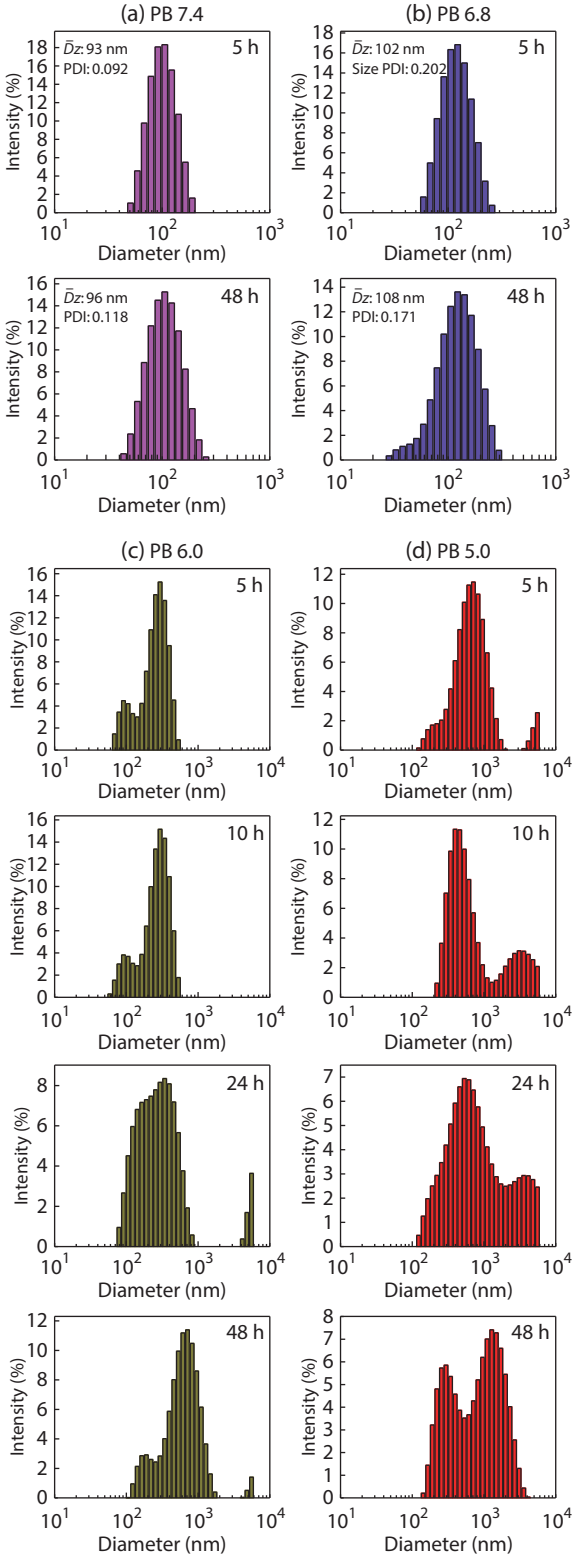

Fig. 5 Particle size distribution histograms of PDNPs (0.5 mg·mL^{-1}) in different pH media: (a) PB 7.4, (b) PB 6.8, (c) PB 6.0 and (d) PB 5.0, as determined by DLS.

the cells are all over 82% no matter the normal cells or the hepatoma carcinoma cells. Therefore, the copolymer H_2N-PEEP-*b*-PBYP has low toxicity to cells and has good biocompatibility. The above results show that polyphosphoester has promising application for drug carriers.

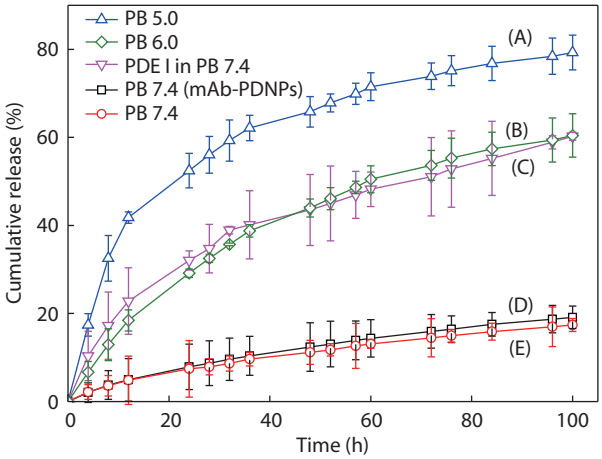

Fig. 6 *In vitro* DOX release curves for (D) mAb-PDNPs in PB 7.4 buffer solution, and PDNPs under different conditions: (A) PB 5.0, (B) PB 6.0, (C) PB 7.4 buffer solution with PDE I, and (E) PB 7.4, respectively. All the sample concentrations were kept at 0.5 mg·mL^{-1} and the temperature at 37 °C.

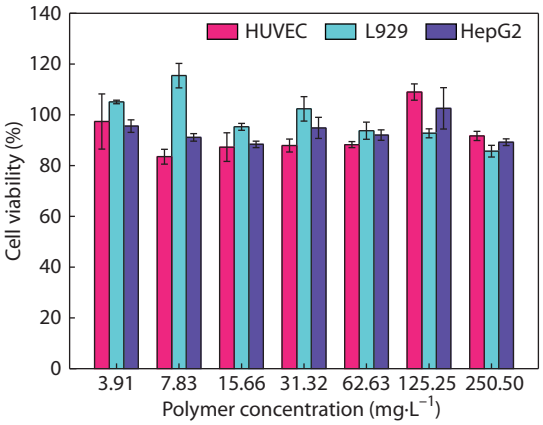

Fig. 7 Cell viability of HUVEC cells, HepG2 cells and L929 cells with H_2N-PEEP$_{64}$-*b*-PBYP$_{36}$ of different concentrations for 48 h incubation.

In Vitro Cytotoxicity

MTT assays were also used to study the cytotoxicity of PDNPs and mAb-PDNPs against HepG2 cells, human cervical cancer cells (HeLa cells) and HUVEC cells, respectively, in which the two later cells have no specific binding sites and can be used as the controls. As shown in Fig. 8(a), after culture HUVEC cells with mAb-PDNPs and PDNPs for 48 h, the cell survival rate was higher, indicating that both mAb-PDNPs and PDNPs hardly released drugs in human healthy cells. In Figs. 8(b) and 8(c), the concentration dependence of the three groups of nanoparticles was observed, that is, the cell viability decreased gradually with the increase of the concentration of nanoparticles. The values of the half maximal inhibitory concentration (IC_{50}) are listed in Table 3, which can be used to evaluate the anti-tumor effect of the nanoparticles. In Fig. 8(b), the IC_{50} values of free DOX, mAb-PDNPs and PDNPs are 0.19, 1.12 and 2.67 mg·L^{-1}, respectively. The mAb-PDNPs show a lower IC_{50} value compared with PDNPs.

https://doi.org/10.1007/s10118-021-2582-3

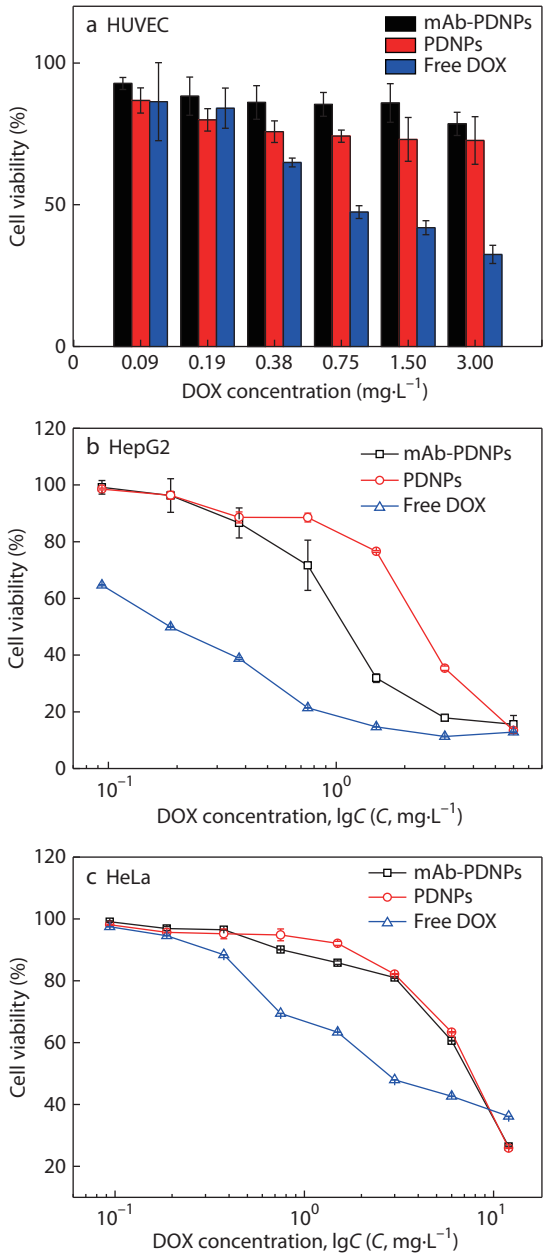

Fig. 8 Cell viabilities of (a) HUVEC cells, (b) HepG2 cells and (c) HeLa cells with mAb-PDNPs, PDNPs and free DOX of different concentrations for 48 h incubation.

Table 3 The IC_{50} values of HepG2 cells and HeLa cells cultured for 48 h with different samples (The IC_{50} value was calculated by GraphPad Prism 8 software).

Sample	IC_{50} for HepG2 (mg·L^{-1})	IC_{50} for HeLa (mg·L^{-1})
mAb-PDNPs	1.12	13.06
PDNPs	2.67	14.25
Free DOX	0.19	4.75

This is due to the fact that mAb-PDNPs can specifically bind to the antigens on the surface of HepG2 cells and promote the enrichment of nanoparticles. On the other hand, compared with the other two groups, free DOX has the lowest IC_{50} value, indicating the highest toxicity. This may be due to the use of polyphosphoester as a drug carrier to reduce the toxicity of the active drug. What is more, since DOX was chemically bound to the polymer, the structure was stable and the bond need to be broken to release DOX into the tumor microenvironment, which takes more time. In Fig. 8(c), the IC_{50} values of PDNPs and mAb-PDNPs are 14.25 and 13.06 mg·L^{-1}, which are similar, because there is no antigen on the surface of HeLa cells that can be specifically recognized with CD147 monoclonal antibody. And the IC_{50} value of free DOX is the lowest of 4.75 mg·L^{-1}, which is similar to that of the case of HepG2 cells in Fig. 8(b). The above results can indicate mAb-PDNPs can realize targeted drug delivery and polyphosphoester as drug carrier can reduce the toxicity of active drug.

Cellular Uptake

It is also important to consider whether the drug-loaded nanoparticles can recognize tumor cells and be internalized by the cells to effectively release the drugs in the tumor cells.[50] Therefore, HepG2 cells and HeLa cells were used to evaluate the cellular uptake for PDNPs and mAb-PDNPs, respectively. A live cell imaging system was used to monitor the uptake process in real time, as shown in Fig. 9. Comparing Fig. 9(a) with Fig. 9(c), DOX fluorescence intensity of mAb-PDNPs is stronger than that of PDNPs in the same period, this is because mAb-PDNPs act on HepG2 cells surface by active targeting, while PDNPs enter the cells by cellular uptake. In addition, as shown in Fig. 9(b), the fluorescence intensity of free DOX is much smaller, because DOX enters the cells through diffusion by virtue of the concentration difference between inside and outside the cells. Besides, by comparing Fig. 9(c) with Fig. 9(f), the fluorescence intensity of HepG2 cells is stronger than that of HeLa cells, because there are antigenic sites on the surface of HepG2 cells that can be targeted and recognized by CD147 monoclonal antibodies. These results show that both nanoparticles could effectively release drug in tumor cells, and mAb-PDNPs possess good targeting ability to HepG2 cells.

CONCLUSIONS

We have proven that the method of binding monoclonal antibodies to polyphosphoester prodrug nanoparticles is a simple and effective system. This technique combines biocompatible and biodegradable polyphosphoesters with anti-tumor drug DOX and CD147 mAb through ring-opening polymerizatin (ROP), click reaction, self-assembly and amidation. It has the functions of targeting specific tumor cells and releasing the original drug to the tumor cell microenvironment. We have characterized the structure and self-assembly behavior of the polymer prodrug H_2N-PEEP-*b*-PBYP-*hyd*-DOX, and the particle size is 93 nm. XPS test proves that the antibody was bonded to the surface of the prodrug nanoparticles, whose particle size increased to 106 nm. We also explored the biocompatibility, stability, environmental responsiveness and drug release of these nanoparticles in different media (pH and phosphatase). The pH-responsive PDNPs could remain relatively stable under the condition of PB 7.4, but quickly dissociated in the tumor microenvironment and finally resulted in the release of DOX. MTT assay and enzymatic degradation tests indicate that the copolymer H_2N-PEEP-*b*-PBYP based on polyphosphoesters

https://doi.org/10.1007/s10118-021-2582-3

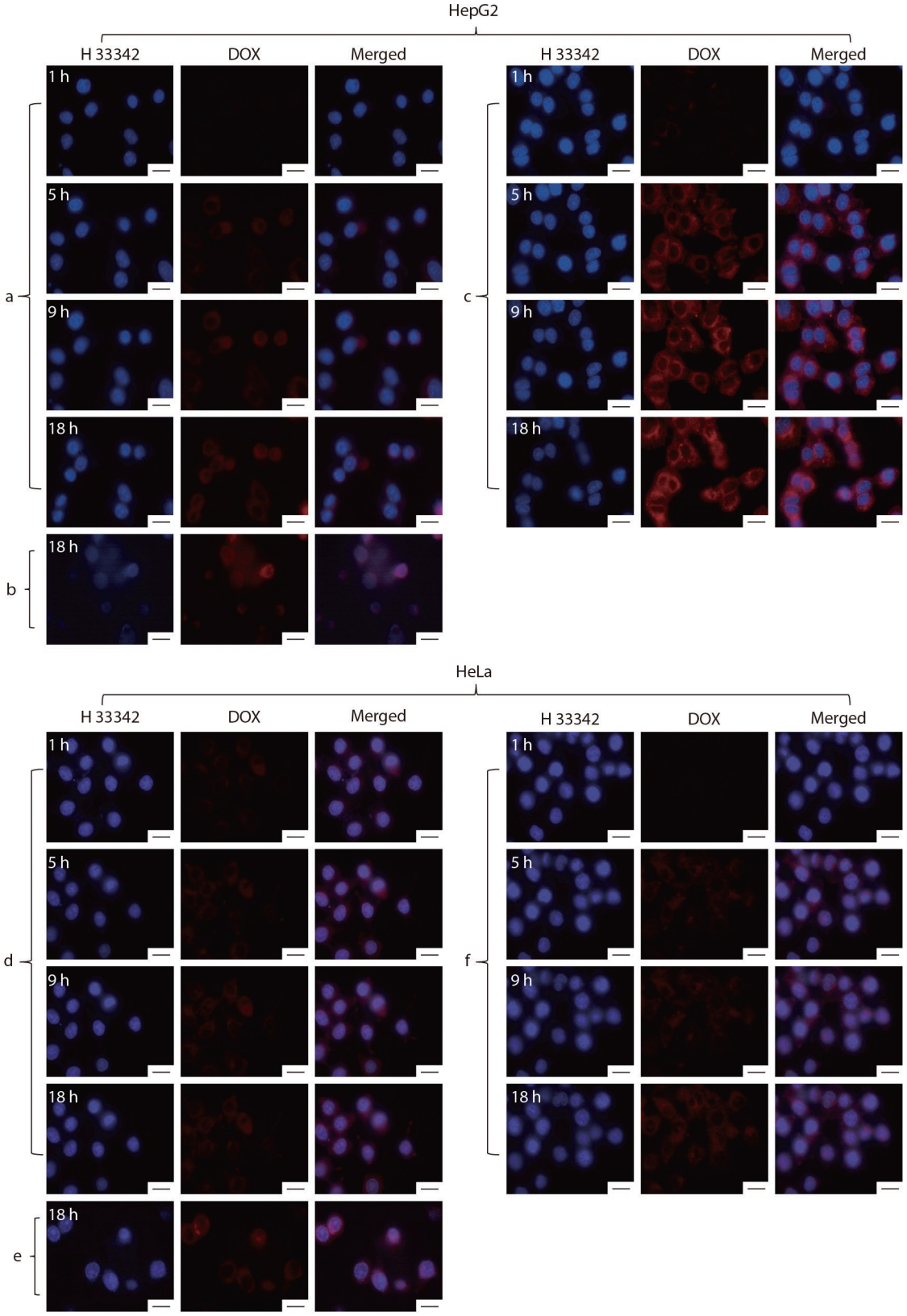

Fig. 9 Live cell imaging system images: HepG2 cells incubated with (a) PDNPs, (b) free DOX and (c) mAb-PDNPs, respectively; HeLa cells incubated with (d) PDNPs, (e) free DOX and (f) mAb-PDNPs, respectively, at different time. For all test, DOX dosage was maintained at 25 mg·L^{-1}. For each group, images from left to right show the cell nuclei stained with H 33342 (blue), the DOX fluorescence in cells (red), and overlays of the two images. All the scale bars of images are 20 μm.

https://doi.org/10.1007/s10118-021-2582-3

possesses favorable biocompatibility and biodegradability. Cytotoxicity assay showed that the mAb-PDNPs could achieve targeted drug delivery for HepG2 cells due to the presence of receptors on the surface of cells. These results will provide a reference preparation method for drug delivery for targeted therapy of liver cancer.

Electronic Supplementary Information

Electronic supplementary information (ESI) is available free of charge in the online version of this article at https://doi.org/10.1007/s10118-021-2582-3

ACKNOWLEDGMENTS

We gratefully acknowledge the financial supports from the National Natural Science Foundation of China (Nos. 21975169 and 21374066), the Natural Science Foundation of Jiangsu Province (No. BK20171212) and a Project Funded by the Priority Academic Program Development (PAPD) of Jiangsu Higher Education Institutions.

REFERENCES

1 Siegel, R. L.; Miller, K. D.; Fuchs, H. E.; Jemal, A. Cancer statistics, 2021. *CA. Cancer J. Clin.* **2021**, *71*, 7–33.
2 Yang, J. D.; Hainaut, P.; Gores, G. J.; Amadou, A.; Plymoth, A.; Roberts, L. R. A global view of hepatocellular carcinoma: trends, risk, prevention and management. *Nat. Rev. Gastroenterol. Hepatol.* **2019**, *16*, 589–604.
3 DeVita, V. T.; Chu, E. A history of cancer chemotherapy. *Cancer Res.* **2008**, *68*, 8643–8653.
4 Wan, X. B.; Zhang, Q.; Chen, M.; Liu, Y. P.; Zheng, J.; Lan, P.; He, F. Prognostic value of interval between the initiation of neoadjuvant treatment to surgery for patients with locally advanced rectal cancer following neoadjuvant chemotherapy, radiotherapy and definitive surgery. *Front. Oncol.* **2020**, *10*, 1280–1290.
5 Chabner, B. A.; Roberts, T. G. Chemotherapy and the war on cancer. *Nat. Rev. Cancer* **2005**, *5*, 65–72.
6 Huang, P.; Wang, D. L.; Su, Y.; Huang, W.; Zhou, Y. F.; Cui, D. X.; Zhu, X. Y., Yan, D. Y. Combination of small molecule prodrug and nanodrug delivery: amphiphilic drug–drug conjugate for cancer therapy. *J. Am. Chem. Soc.* **2014**, *136*, 11748–11756.
7 Strebhardt, K.; Ullrich, A. Paul Ehrlich's magic bullet concept: 100 years of progress. *Nat. Rev. Cancer* **2008**, *8*, 473–480.
8 Khongorzul, P.; Ling, C. J.; Khan, F. U.; Ihsan, A. U.; Zhang, J. Antibody-drug conjugates: a comprehensive review. *Mol. Cancer Res.* **2020**, *18*, 3–19.
9 Tsuchikama, K.; An, Z. Q. Antibody-drug conjugates: recent advances in conjugation and linker chemistries. *Protein & Cell* **2018**, *9*, 33–46.
10 Joubert, N.; Beck, A.; Dumontet, C.; Denevault-Sabourin, C. Antibody-drug conjugates: the last decade. *Pharmaceuticals* **2020**, *13*, 245–275.
11 Beck, A.; Goetsch, L.; Dumontet, C.; Corvaia, N. Strategies and challenges for the next generation of antibody–drug conjugates. *Nat. Rev. Drug Discovery* **2017**, *16*, 315–337.
12 Tumey, L. N.; Charati, M.; He, T.; Sousa, E.; Ma, D. S.; Han, X. G.; Clark, T.; Casavant, J.; Loganzo, F.; Barletta, F.; Lucas, J.; Graziani, E. I. Mild method for succinimide hydrolysis on ADCs: impact on ADC potency, stability, exposure, and efficacy. *Bioconjug. Chem.* **2014**, *25*, 1871–1880.
13 Trail, P. A.; Dubowchik, G. M.; Lowinger, T. B. Antibody drug conjugates for treatment of breast cancer: novel targets and diverse approaches in ADC design. *Pharmacol. Ther.* **2018**, *181*, 126–142.
14 Frutos, S.; Hernandez, J. L.; Otero, A.; Calvis, C.; Adan, J.; Mitjans, F.; Vila-Perello, M. Site-specific antibody drug conjugates using streamlined expressed protein ligation. *Bioconjug. Chem.* **2018**, *29*, 3503–3508.
15 Shen, Y. Q.; Jin, E.; Zhang, B.; Murphy, C. J.; Sui, M.; Zhao, J.;Wang. J. Q.; Tang, J. Q.; Fan, M. H.; Kirk, E. V.; Murdoch, W. J. Prodrugs forming high drug loading multifunctional nanocapsules for intracellular cancer drug delivery. *J. Am. Chem. Soc.* **2010**, *132*, 4259–4265.
16 Denny, W. A. Prodrug strategies in cancer therapy. *Eur. J. Med. Chem.* **2011**, *36*, 577–595.
17 Chen, H. B.; Gu, Z. J.; An, H. W.; Chen, C. Y.; Chen, J.; Cui, R.; Chen, S. Q.; Chen, W. H.; Chen, X. S.; Chen, X. Y.; Chen, Z.; Ding, B. Q.; Dong, Q.; Fan, Q.; Fu, T.; Hou, D. Y.; Jiang, Q.; Ke, H. T.; Jiang, X. Q.; Liu, G.; Li, S. P.; Li, T. Y.; Liu, Z.; Nie, G. J.; Ovais, M.; Pang, D. W.; Qiu, N. S.; Shen, Y. Q.; Tian, H. Y.; Wang, C.; Wang, H.; Wang, Z. Q.; Xu, H. P.; Xu, J. F.; Yang, X. L.; Zhu, S.; Zheng, X. C.; Zhang, X. Z.; Zhao, Y. B.; Tan, W. H.; Zhang, X.; Zhao, Y. L. Precise nanomedicine for intelligent therapy of cancer. *Sci. China Chem.* **2018**, *61*, 1503–1552.
18 Qiu, M.; Ouyang, J.; Wei, Y. H.; Zhang, J.; Lan, Q.; Deng, C.; Zhong, Z. Y. Selective cell penetrating peptide-functionalized envelope-type chimeric lipopepsomes boost systemic RNAi therapy for lung tumors. *Adv. Healthc. Mater.* **2019**, *8*, 1900500–1900508.
19 Li, D.; Su, T. Q.; Ma, L. L.; Yin, F.; Xu, W. G.; Ding, J. X.; Li, Z. G. Dual-acidity-labile polysaccharide-di-drugs conjugate for targeted cancer chemotherapy. *Eur. J. Med. Chem.* **2020**, *199*, 112367.
20 Jiang, Z. Y.; Feng, X. R.; Xu, W. G.; Zhuang, X. L.; Ding, J. X.; Chen, X. S. Calcium phosphate-cured nanocluster of poly(L-glutamic acid)-cisplatin and arsenic trioxide for synergistic chemotherapy of peritoneal metastasis of ovarian cancer. *Acta Polymerica Sinica* (in Chinese) **2020**, *51*, 901–910.
21 Li, Y.; Li, Y. H.; Ji, W. H.; Lu, Z. G.; Liu, L. Y.; Shi, Y. J. Ma, G. H.; Zhang, X. Positively charged polyprodrug amphiphiles with enhanced drug loading and ROS-responsive release ability for traceable synergistic therapy. *J. Am. Chem. Soc.* **2018**, *140*, 4164–4171.
22 Wang, Y. S.; Li, G. L.; Zhu, S. B.; Jing, F. C.; Liu, R. D.; Li, S. S.; He, J.; Lei, J. D. A self-assembled nanoparticle platform based on amphiphilic oleanolic acid polyprodrug for cancer therapy. *Chinese J. Polym. Sci.* **2020**, *38*, 819–829.
23 Hu, X. L.; Hu, J. M.; Tian, J.; Ge, Z. S.; Zhang, G. Y.; Luo, K. F.; Liu, S. Y. Polyprodrug amphiphiles: hierarchical assemblies for shape-regulated cellular internalization, trafficking, and drug delivery. *J. Am. Chem. Soc.* **2013**, *135*, 17617–17629.
24 Hu, X. L.; Liu, G. H.; Li, Y.; Wang, X. R.; Liu, S. Y. Cell-penetrating hyperbranched polyprodrug amphiphiles for synergistic reductive milieu-triggered drug release and enhanced magnetic resonance signals. *J. Am. Chem. Soc.* **2015**, *137*, 362–368.
25 Zhou, Q.; Shao, S. Q.; Wang, J. Q.; Xu, C. H.; Xiang, J. J.; Piao, Y.; Zhou, Z. X.; Yu, Q. S.; Tang, J. B.; Liu, X. R.; Gan, Z. H.; Mo, Ran.; Gu, Z.; Shen, Y. Q. Enzyme-activatable polymer–drug conjugate augments tumour penetration and treatment efficacy. *Nat. Nanotechnol.* **2019**, *14*, 799–809.
26 Hao, Q. B.; Wang, Z. X.; Zhao, W.; Wen, L. W.; Wang, W. H.; Lu, S. Y.; Xing, D.; Zhan, M. X.; Hu, X. L. Dual-responsive polyprodrug nanoparticles with cascade-enhanced magnetic resonance signals for deep-penetration drug release in tumor therapy. *ACS Appl. Mater. Interfaces* **2020**, *12*, 49489–49501.
27 Kocbek, P.; Obermajer, N.; Cegnar, M.; Kos, J.; Kristl, J. Targeting cancer cells using PLGA nanoparticles surface modified with

monoclonal antibody. *J. Control. Release* **2007**, *120*, 18–26.
28 Son, S.; Shin, S.; Rao, N. V.; Um, W.; Jeon, J.; Ko, H.; Deepagan, V. G.; Kwon, S.; Lee, J. Y.; Park, J. H. Anti-Trop2 antibody-conjugated bioreducible nanoparticles for targeted triple negative breast cancer therapy. *Int. J. Biol. Macromol.* **2018**, *110*, 406–415.
29 Wan, J. X.; Li, Y. J.; Jin, K.; Guo, J.; Xu, J. T.; Wang, C. C. Robust strategy for antibody-polymer-drug conjugation: significance of conjugating orientation and linker charge on targeting ability. *ACS Appl. Mater. Interfaces* **2020**, *12*, 23717–23725.
30 Song, Y.; Li, D.; He, J. L.; Zhang, M. Z.; Ni, P. H. Facile preparation of pH-responsive PEGylated prodrugs for activated intracellular drug delivery. *Chin. Chem. Lett.* **2019**, *30*, 2027–2031.
31 Zuo, C.; Peng, J. L.; Cong, Y.; Dai, X. Y.; Zhang, X. L.; Zhao, S. J.; Zhang, X. S.; Ma, L. W.; Wang, B. Y.; Wei, H. Fabrication of supramolecular star-shaped amphiphilic copolymers for ROS-triggered drug release. *J. Colloid. Interface* **2018**, *514*, 122–131.
32 Zhu, Y. Q.; Zhang, J.; Meng, F. H.; Cheng, L.; Feijen, J.; Zhong, Z. Y. Reduction-responsive core-crosslinked hyaluronic acid-*b*-poly(trimethylene carbonate-*co*-dithiolane trimethylene carbonate) micelles: synthesis and CD44-mediated potent delivery of docetaxel to triple negative breast tumor in vivo. *J. Mater. Chem. B* **2018**, *6*, 3040–3047.
33 Jin, H.; Zhu, T.; Huang, X. G.; Sun, M.; Li, H. G.; Zhu, X. Y.; Liu, M. L.; Xie, Y. B.; Huang, W.; Yan, D. Y. ROS-responsive nanoparticles based on amphiphilic hyperbranched polyphosphoester for drug delivery: light-triggered size-reducing and enhanced tumor penetration. *Biomaterials* **2019**, *211*, 68–80.
34 Chu, C. Y.; Lyu, X. M.; Wang, Z. X.; Jin, H.; Lu, S. Y.; Xing, D.; Hu, X. L. Cocktail polyprodrug nanoparticles concurrently release cisplatin and peroxynitrite-generating nitric oxide in cisplatin-resistant cancers. *Chem. Eng. J.* **2020**, *402*, 126125–126155.
35 Liu, T. Zhang, Y. F.; Liu, S. Y. Drug and plasmid DNA co-delivery nanocarriers based on ABC-type polypeptide hybrid miktoarm star copolymers. *Chinese J. Polym. Sci.* **2013**, *31*, 924–937.
36 Zhang, G. Y.; Zhang, M. Z.; He, J. L.; Ni, P. H. Synthesis and characterization of a new multifunctional polymeric prodrug paclitaxel-polyphosphoester-folic acid for targeted drug delivery. *Polym. Chem.* **2013**, *4*, 4515–4525.
37 Ma, G. Q.; Liu, J.; He, J. L.; Zhang, M. Z.; Ni, P. H. Dual-responsive polyphosphoester-doxorubicin prodrug containing diselenide bond: synthesis, characterization and drug delivery. *ACS Biomater. Sci. Eng.* **2018**, *4*, 2443–2452.
38 Dong, S. X.; Sun, Y.; Liu, J.; Li, L.; He, J. L.; Zhang, M. Z.; Ni, P. H. Multifunctional polymeric prodrug with simultaneous conjugating camptothecin and doxorubicin for pH/reduction dual-responsive drug delivery. *ACS Appl. Mater. Interfaces* **2019**, *11*, 8740–8748.
39 Xu, S. J.; Cui, F. B.; Huang, D. F.; Zhang, D. H.; Zhu, A. Q.; Sun, X.; Cao, Y. M.; Ding, S.; Wang, Y.; Gao, E. Y.; Zhang, F. L. PD-L1 monoclonal antibody-conjugated nanoparticles enhance drug delivery level and chemotherapy efficacy in gastric cancer cells. *Int. J. Nanomed.* **2019**, *14*, 17–32.
40 Zheng, P.; Liu, Y.; Chen, J. J.; Xu, W. G.; Li, G.; Ding, J. X. Targeted pH-responsive polyion complex micelle for controlled intracellular drug delivery. *Chin. Chem. Lett.* **2020**, *31*, 1178–1182.
41 Fu, F. F.; Zhou, B. Q.; Ouyang, Z. J.; Wu, Y. L.; Zhu, J. Y. Shen, M. W.; Xia, J. D.; Shi, X. Y. Multifunctional cholesterol-modified dendrimers for targeted drug delivery to cancer cells expressing folate receptors. *Chinese J. Polym. Sci.* **2019**, *37*, 129–135.
42 Toole, B. P. Emmprin (CD147), a cell surface regulator of matrix metalloproteinase production and function. *Curr. Top. Dev. Biol.* **2003**, *54*, 371–389.
43 Qu, C. X.; Li, J. Z.; Zhou, Y. J.; Yang, S. D.; Chen, W. L.; Li, F.; You, B. G.; Liu, Y.; Zhang, X. N. Targeted delivery of doxorubicin *via* CD147-mediated ROS/pH dual-sensitive nanomicelles for the efficient therapy of hepatocellular carcinoma. *AAPS J.* **2018**, *20*, 34–47.
44 Wang, J.; Wu, Z. T.; Pan, G. Y.; Ni, J. S.; Xie, F. Y.; Jiang, B. G.; Wei, L. X.; Gao, J.; Zhou, W. P. Enhanced doxorubicin delivery to hepatocellular carcinoma cells *via* CD147 antibody-conjugated immunoliposomes. *Nanomedicine* **2018**, *14*, 1949–1961.
45 Huang, P.; Wang, G. C.; Su, Y.; Zhou, Y. F.; Huang, W.; Zhang, R.; Yan, D. Y. Stimuli-responsive nanodrug self-assembled from amphiphilic drug-inhibitor conjugate for overcoming multidrug resistance in cancer treatment. *Theranostics* **2019**, *9*, 5755–5768.
46 Chan, J. M. W.; Tan, J. P. K.; Engler, A. C.; Ke, X. Y.; Gao, S. J.; Yang, C.; Sardon, H.; Yang, Y. Y.; Hedrick, J. L. Organocatalytic anticancer drug loading of degradable polymeric mixed micelles *via* a biomimetic mechanism. *Macromolecules* **2016**, *49*, 2013–2021.
47 Li, S. Y.; Liu, L. H.; Jia, H. Z.; Qiu, W. X.; Rong, L.; Cheng, H.; Zhang, X. Z. A pH-responsive prodrug for real-time drug release monitoring and targeted cancer therapy. *Chem. Commun.* **2014**, *50*, 11852–11855.
48 Mao, J.; Li, Y.; Wu, T.; Yuan, C. H.; Zeng, B. R.; Xu, Y. T.; Dai, L. Z. A simple dual-pH responsive prodrug-based polymeric micelle for drug delivery. *ACS Appl. Mater. Interfaces* **2016**, *8*, 17109–17117.
49 Li, L.; Li, D.; Zhang, M. Z.; He, J. L.; Liu, J.; Ni, P. H. One-pot synthesis of pH/redox responsive polymeric prodrug and fabrication of shell cross-linked prodrug micelles for antitumor drug transportation. *Bioconjug. Chem.* **2018**, *29*, 2806–2817.
50 Zhao, K. D.; Li, D. Xu, W. G.; Ding, J. X.; Jiang, W. Q.; Li, M. Q.; Wang, C. X.; Chen, X. S. Targeted hydroxyethyl starch prodrug for inhibiting the growth and metastasis of prostate cancer. *Biomaterials* **2017**, *116*, 82–94.

https://doi.org/10.1007/s10118-021-2582-3